

Communication

Electrochemical Switching of First-Generation Donor-Acceptor Stenhouse Adducts (DASAs): An Alternative Stimulus for Triene Cyclisation

Nicholas D. Shepherd¹, Harrison S. Moore¹, Jonathon E. Beves² and Deanna M. D'Alessandro^{1,*}

¹ School of Chemistry, The University of Sydney, Sydney, NSW 2006, Australia; nshe0025@uni.sydney.edu.au (N.D.S.); hmoo4552@uni.sydney.edu.au (H.S.M.)

² School of Chemistry, The University of New South Wales, Sydney, NSW 2052, Australia; j.beves@unsw.edu.au

* Correspondence: deanna.dalessandro@sydney.edu.au

Abstract: Donor-acceptor Stenhouse adducts (DASAs) are a photo-switch class that undergoes triene cyclisation in response to visible light. Herein, electrochemical oxidation is demonstrated as an effective alternative stimulus for the triene cyclisation commonly associated with photo-switching.

Keywords: photoswitching; electrochemistry; stimuli responsive



Citation: Shepherd, N.D.; Moore, H.S.; Beves, J.E.; D'Alessandro, D.M. Electrochemical Switching of First-Generation Donor-Acceptor Stenhouse Adducts (DASAs): An Alternative Stimulus for Triene Cyclisation. *Chemistry* **2021**, *3*, 728–733. <https://doi.org/10.3390/chemistry3030051>

Academic Editor: Catherine Housecroft

Received: 23 February 2021

Accepted: 28 June 2021

Published: 7 July 2021

Publisher's Note: MDPI stays neutral with regard to jurisdictional claims in published maps and institutional affiliations.



Copyright: © 2021 by the authors. Licensee MDPI, Basel, Switzerland. This article is an open access article distributed under the terms and conditions of the Creative Commons Attribution (CC BY) license (<https://creativecommons.org/licenses/by/4.0/>).

Organic photo-switches have gained significant attention due to the contrasting properties of their initial and metastable states [1]. Accessing these states via controlled light irradiation allows efficient modulation of their properties which are relevant to applications including chemical sensing [2,3], drug delivery [2,3], heterogenous catalysis [4], molecular machines [5,6], and data storage [7].

Donor-acceptor Stenhouse adducts (DASAs) [8–12] are a class of photo-switches that are visible light-responsive, thus minimising photochemical degradation [13]. DASAs are comprised of donor (provided by the nucleophile used during synthesis) and acceptor (provided by a carbon acid, usually Meldrum's or 1,3-dimethyl barbituric acids) components linked by a central triene chain (Figure 1c–h) [8–10]. Typically, excitation with white light results in triene chain's cyclisation to yield a cyclopentenone zwitterionic species (Figure 2d) [8–10]. Further appeal for this photo-switch class is based on the relatively simple two-step synthetic procedure [10]. Syntheses detailed in the literature involve the preparation of an activated furan precursor through Knoevenagel condensation between a carbon acid and furan [8–10]. The respective DASA is completed through nucleophilic addition of the respective donor component [8–10]. In addition to the aforementioned applications [14–16], DASAs have also been used in preparing orthogonal photo-switches [17] and photolithography [18,19].

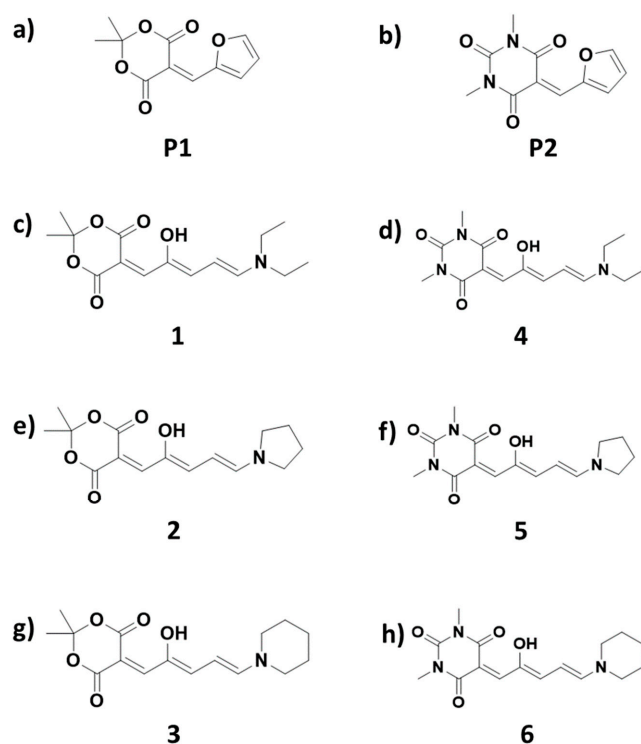


Figure 1. First-generation DASA compounds were prepared from precursors P1 and P2 (a,b, respectively). DASAs subject to voltammetry and UV-vis SEC analyses are designated as 1–6 (c–h).

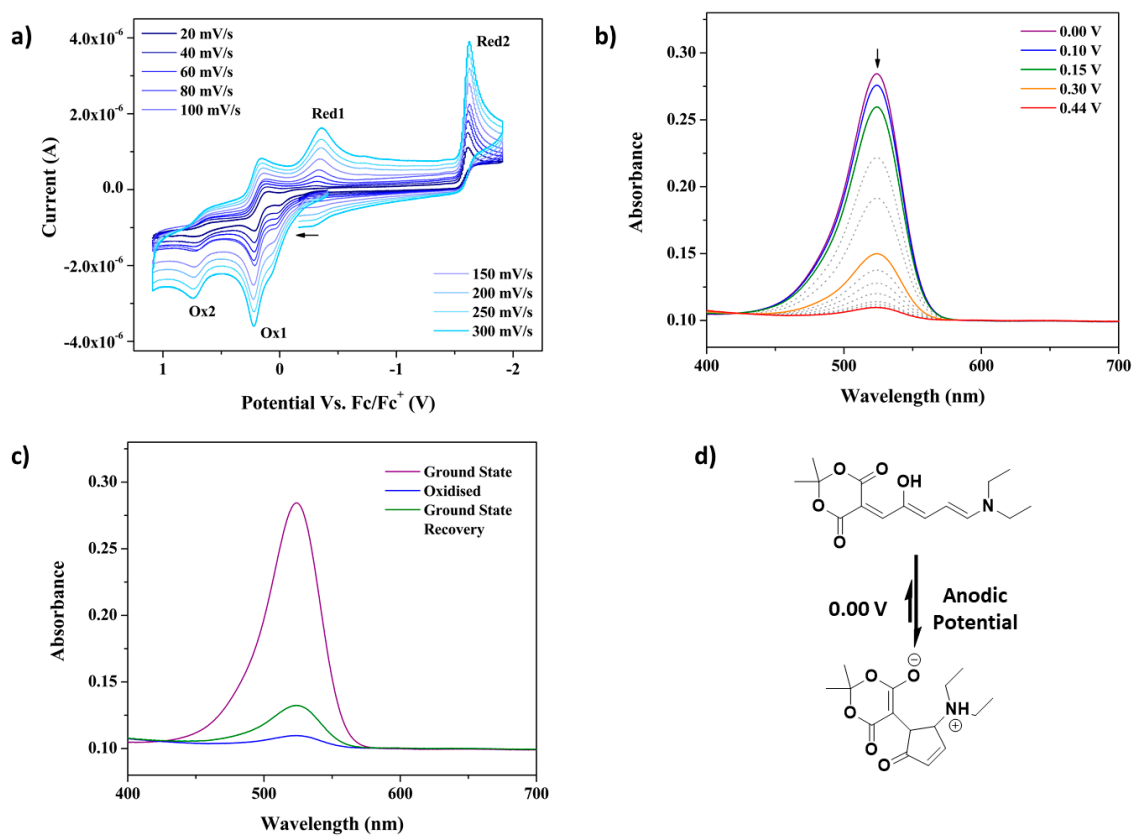


Figure 2. CV recorded at 20–300 mV/s scan rates (a); UV-vis SEC spectra from 400–700 nm (14,250–25,750 cm⁻¹) (b); UV-vis spectra following SEC indicating recovery of the linear isomer in the same range (arrow shows the direction of change) (c); and proposed quasi-reversible cyclisation in response to an anodic redox potential (d) for compound 1. Electrochemical experiments were conducted in 0.1 M TBAPF₆ in MeCN.

While most DASA studies have focused on photo-switching behaviour, acidic and basic conditions have been shown to stabilise the metastable state [15,20]. Furthermore, other organic photo-switch classes have responded to alternative stimuli such as heating [21,22], pH [21,22], and redox potential [21–26]. In particular, select azobenzene [25,26], chromene [23,24,27,28], and diarylethene [29,30] photo-switches can undergo their photo-switching behaviour in response to an applied redox potential.

Herein, a series of first-generation DASA compounds (denoted 1–6 in Figure 1) were subjected to voltammetric and UV-vis spectroelectrochemical (UV-vis SEC) studies to elucidate their redox activity and establish the potential for electrochemical switching. These inquiries were expected to demonstrate a link with photo-controlled DASA cyclisation. DASAs included structures prepared from P1 and P2 precursors, as shown in Figure 1.

DASA compounds and their precursors were prepared in accordance with procedures from the literature [8,9]. Successful syntheses were confirmed using ^1H NMR (ESI, Figures S1–S8), ESI-MS (ESI, Figures S9–S16), and ATR-FTIR (ESI, Figures S17–S24) spectroscopies. UV-vis spectra (ESI, Figures S25–S30) in MeCN indicated a transition in the visible region for 1–6. This signal was consistent with the S_0 – S_1 transition associated with the respective DASAs' triene chain [8–10]. λ_{max} was considerably higher for compounds prepared from 1,3-dimethyl barbituric acid instead of Meldrum's acid (1: 524 nm, 2: 526 nm, and 3: 523 nm, compared to 4: 549 nm, 5: 552 nm, and 6: 548 nm). As expected, the peak intensity decreased following irradiation with white LEDs (4 Watts) as a result of expected photo-switching behaviour [8–10]. Compound 2 was the only DASA that exhibited near quantitative conversion in MeCN, based on the S_0 – S_1 transition intensity reducing by ca. 98%. Other DASA species underwent incomplete photo-switching in MeCN (ca. 68–87%) based on the partial disappearance of the S_0 – S_1 band. Spectral changes following photo-irradiation in MeCN were irreversible.

Cyclic and square wave voltammetry (CV and SQW, respectively) for 1–6 (Figure 2a and ESI, Figures S31–S36) indicated two quasi-reversible oxidation processes of interest. These were designated as Ox1 and Ox2 with average $E_{1/2}$ values of ca. 0.117 and 0.680 V (ESI, Table S1), respectively. Oxidation processes were consistent with the 4π -electrocyclisation step where the alcohol functional group was oxidised as part of the photo-switching mechanism [31]. It is expected that the electrolyte would stabilise the zwitterionic state as observed in redox active spiroopyran functional groups [24]. $E_{1/2}$ values for Ox1 and Ox2 were higher in DASAs 1–3 compared to 4–6. This was attributed to the carbon acid (either Meldrum's or 1,3-dimethylbarbituric acid), where a reduced electron withdrawing effect in 4–6 promoted electron transfer [8,10,32]. The exceptions were compounds 3 and 6, where the latter had a higher $E_{1/2}$ compared to the former. Additionally, $E_{1/2}$ values for Ox1 varied based on the amine derivative used. Potentials increased for DASAs derived from piperidine (3: 0.118, 6: 0.0355 V), pyrrolidine (2: 0.166 V, 5: 0.0840 V), and Et_2NH (1: 0.190 V, 4: 0.111 V) nucleophiles. The electron-donating effects of the donor component of 1–6 was expected to reduce $E_{1/2}$ based on documented nucleophile effects on DASA photo-switching wavelengths [8,10,32]. Scan rate dependence plots for Ox1 and Ox2 indicated that these processes were affected by diffusion (ESI, Figures S39–S44). Red2 in 1–6 was consistent with redox processes associated with P1 and P2 precursors (ESI, Figures S37–S38 and Table S1) and were not attributed to the triene cyclisation.

UV-vis SEC measurements linked electrochemical oxidation processes to the triene cyclisation. Applying an anodic potential resulted in a decrease in the S_0 – S_1 band intensity in all DASA compounds, with representative data for 1 provided in Figure 2b (see also ESI, Figures S45a–S49a). The trends in $E_{1/2}$ values calculated for 1–6 from voltammetric experiments were consistent with the potentials required for electrochemical oxidation during SEC experiments (ESI, Table S2).

The spectral behaviour noted during UV-vis SEC experiments indicated complete conversion to the cyclised state following application of a potential, compared to typically incomplete switching under photo-irradiation. The reduction in S_0 – S_1 band intensity in response to an anodic potential also indicated that it was a more effective stimulus than

photo-irradiation. Most DASA compounds studied herein showed a more substantial decrease in band intensity during SEC experiments. Photo-switching was likely, in part, hindered by the DASA concentration, as outlined by Lui et al. [33] for DASAs in chloroform and toluene solvents. This would be compounded by MeCN being a polar solvent that has inhibited switching behaviour in past studies [11]. In this respect, an anodic potential was able to overcome these impediments, as both switching experiments in the current work were conducted at approximately the same concentration. Additionally, the charge carrier effect of the electrolyte likely further enhances the efficiency of DASA cyclisation via electrochemical oxidation. The main exception was compound **6**, where photo-irradiation (ca. 87% conversion) was more effective than electrochemical oxidation (ca. 77% conversion) at inducing cyclisation. Additionally, for compound **2**, both stimuli resulted in nearly quantitative yield of the cyclised state. It is likely that this is in part attributable to the electron donating nature of the respective nucleophile [34], although this will require further investigation for confirmation.

Removing the potential resulted in a partial return of the S_0 - S_1 band (Figure 2c and ESI, Figure S45b–Figure S49b), in keeping with quasi-reversible behaviour observed in CV data. The reappearance of the S_0 - S_1 band also suggests that the Red1 peak detected in CV data for **1–6** (Figure 1a and ESI, Figures S31–S36) was associated with a reduction in the linear isomer. Note the discrepancy between voltammetry and SEC voltages is due to the Fc/Fc⁺ internal reference in CV experiments. Recovery ranged from 4–47% recovery (ESI, Table S2) across the series, with 4 and 3 representing the lower and upper limits, respectively. It was further noted that the nucleophile appeared to affect recovery, where Et₂NH < pyrrolidine < piperidine (ESI, Table S2). Trends in recovery were also attributed to the electron withdrawing effect of the carbon acid as noted previously [8,10,32]. It was expected that the electron withdrawing behaviour of the acceptor component would adversely affect reversibility. Additionally, the diminished fatigue resistance compared to that observed in photo-switching studies [9] is also attributable to the harsh nature associated with an electrochemical potential.

The SEC data confirmed that application of an anodic potential resulted in the conversion of the linear isomer to the cyclised zwitterion (Figure 2d). Similar behaviour has also been observed in spiropyran-based materials where the electrolyte stabilises the zwitterionic merocyanine species [24]. The immediate decrease in S_0 - S_1 band intensity confirmed that the Ox1 processes in **1–6** were associated with the 4π -electrocyclisation step, precluding a multistep process as observed during photo-switching [31,35]. The initial conversion demonstrated an alternative stimulus for DASA switching. The poor recovery of the linear configuration following electrochemical oxidation indicates exposure to this stimulus would impede long-term switching function during practical applications. Therefore, compounds and materials with improved fatigue resistance are necessary to exploit this switching behaviour in a functional context.

In summary, selected first-generation DASAs exhibited the cyclisation traditionally associated with their photo-switching behaviour in response to an anodic potential. Furthermore, electrochemical oxidation was demonstrated to be more effective than photo-irradiation for cyclising most of the DASAs studied in the current work. Despite this, the alternative stimulus was only partially effective, with poor recovery of the linear triene isomer. This work points to the potential for electrochemical switching of DASA-incorporated systems of interest for electrochemical sensing, electrocatalysis, and electrochemically driven molecular machines. These studies are currently underway in our laboratory.

Supplementary Materials: The following are available online at <https://www.mdpi.com/article/10.3390/chemistry3030051/s1>, Figures S1–S8: NMR data, Figures S9–S16: ESI-MS data, Figures S17–S24: ATR-FTIR data, Figures S25–S30: UV-Vis spectra from 400–700 nm, Figures S31–S38: CV data, Figures S39–S44: Scan rate dependence data, Figures S45–S49: Spectroelectrochemical data, Tables S1 and S2: Redox processes for DASAs and precursors.

Author Contributions: N.D.S. completed the experimental work and compiled the manuscript. H.S.M. and J.E.B. provided collaborative support with the measurement and interpretation of data. D.M.D. supervised the overall project. All authors have read and agreed to the published version of the manuscript.

Funding: Australian Research Council for funding (FT170100283, FT170100094) as well as the University of Sydney (USyd) for support.

Data Availability Statement: Data available on request from the corresponding author.

Acknowledgments: The authors would like to thank the Australian Research Council for funding (FT170100283, FT170100094) as well as the University of Sydney (USyd) for support. N.D.S. gratefully acknowledges the School of Chemistry, USyd for support provided by the 'Postgraduate Scholarship for Photoactive Metal-Organic Frameworks'.

Conflicts of Interest: The authors declare no conflict of interest.

References

1. Natali, M.; Giordani, S. Molecular Switches as Photocontrollable "Smart" Receptors. *Chem. Soc. Rev.* **2012**, *41*, 4010–4029. [[CrossRef](#)]
2. Tylkowski, B.; Trojanowska, A.; Marturano, V.; Nowak, M.; Marciniak, L.; Giamberini, M.; Ambrogi, V.; Cerruti, P. Power of Light—Functional Complexes Based on Azobenzene Molecules. *Coord. Chem. Rev.* **2017**, *351*, 205–217. [[CrossRef](#)]
3. Avella-Oliver, M.; Morais, S.; Puchades, R.; Maquieira, Á. Towards Photochromic and Thermochromic Biosensing. *TrAC-Trends Anal. Chem.* **2016**, *79*, 37–45. [[CrossRef](#)]
4. Gong, L.L.; Yao, W.T.; Liu, Z.Q.; Zheng, A.M.; Li, J.Q.; Feng, X.F.; Ma, L.F.; Yan, C.S.; Luo, M.B.; Luo, F. Photoswitching Storage of Guest Molecules in Metal-Organic Framework for Photoswitchable Catalysis: Exceptional Product, Ultrahigh Photocontrol, and Photomodulated Size Selectivity. *J. Mater. Chem. A* **2017**, *5*, 7961–7967. [[CrossRef](#)]
5. Terao, F.; Morimoto, M.; Irie, M. Light-Driven Molecular-Crystal Actuators: Rapid and Reversible Bending of Rodlike Mixed Crystals of Diarylethene Derivatives. *Angew. Chemie-Int. Ed.* **2012**, *51*, 901–904. [[CrossRef](#)]
6. Feringa, B.L. In Control of Motion: From Molecular Switches to Molecular Motors. *Acc. Chem. Res.* **2001**, *34*, 504–513. [[CrossRef](#)]
7. Andréasson, J.; Pischel, U. Storage and Processing of Information Using Molecules: The All-Photonic Approach with Simple and Multi-Photochromic Switches. *Isr. J. Chem.* **2013**, *53*, 236–246. [[CrossRef](#)]
8. Helmy, S.; Oh, S.; Leibfarth, F.A.; Hawker, C.J.; Read De Alaniz, J. Design and Synthesis of Donor-Acceptor Stenhouse Adducts: A Visible Light Photoswitch Derived from Furfural. *J. Org. Chem.* **2014**, *79*, 11316–11329. [[CrossRef](#)] [[PubMed](#)]
9. Helmy, S.; Leibfarth, F.; Oh, S.; Poelma, J.; Hawker, C.J.; Read De Alaniz, J. Photoswitching Using Visible Light: A New Class of Organic Photochromic Molecules. *J. Am. Chem. Soc.* **2014**, *136*, 8169–8172. [[CrossRef](#)]
10. Lerch, M.M.; Szymański, W.; Feringa, B.L. The (Photo)Chemistry of Stenhouse Photoswitches: Guiding Principles and System Design. *Chem. Soc. Rev.* **2018**, *47*, 1910–1937. [[CrossRef](#)] [[PubMed](#)]
11. Mallo, N.; Foley, E.D.; Iranmanesh, H.; Kennedy, A.D.W.; Luis, E.T.; Ho, J.; Harper, J.B.; Beves, J.E. Structure-Function Relationships of Donor-Acceptor Stenhouse Adduct Photochromic Switches. *Chem. Sci.* **2018**, *9*, 8242–8252. [[CrossRef](#)]
12. Mallo, N.; Tron, A.; Andréasson, J.; Harper, J.B.; Jacob, L.S.D.; McClenaghan, N.D.; Jonusauskas, G.; Beves, J.E. Hydrogen-Bonding Donor-Acceptor Stenhouse Adducts. *ChemPhotoChem* **2020**, *4*, 407–412. [[CrossRef](#)]
13. Bléger, D.; Hecht, S. Visible-Light-Activated Molecular Switches. *Angew. Chemie-Int. Ed.* **2015**, *54*, 11338–11349. [[CrossRef](#)]
14. Poelma, S.O.; Oh, S.S.; Helmy, S.; Knight, A.S.; Burnett, G.L.; Soh, H.T.; Hawker, C.J.; Read De Alaniz, J. Controlled Drug Release to Cancer Cells from Modular One-Photon Visible Light-Responsive Micellar System. *Chem. Commun.* **2016**, *52*, 10525–10528. [[CrossRef](#)] [[PubMed](#)]
15. Zhong, D.; Cao, Z.; Wu, B.; Zhang, Q.; Wang, G. Polymer Dots of DASA-Functionalized Polyethyleneimine: Synthesis, Visible Light/PH Responsiveness, and Their Applications as Chemosensors. *Sensors Actuators, B Chem.* **2018**, *254*, 385–392. [[CrossRef](#)]
16. Balamurugan, A.; Lee, H. A Visible Light Responsive On–Off Polymeric Photoswitch for the Colorimetric Detection of Nerve Agent Mimics in Solution and in the Vapor Phase. *Macromolecules* **2016**, *49*, 2568–2574. [[CrossRef](#)]
17. Lerch, M.M.; Hansen, M.J.; Velema, W.A.; Szymanski, W.; Feringa, B.L. Orthogonal Photoswitching in a Multifunctional Molecular System. *Nat. Commun.* **2016**, *7*, 1–10. [[CrossRef](#)] [[PubMed](#)]
18. Sinawang, G.; Wu, B.; Wang, J.; Li, S.; He, Y. Polystyrene Based Visible Light Responsive Polymer with Donor–Acceptor Stenhouse Adduct Pendants. *Macromol. Chem. Phys.* **2016**, *217*, 2409–2414. [[CrossRef](#)]
19. Singh, S.; Friedel, K.; Himmerlich, M.; Lei, Y.; Schlingloff, G.; Schober, A. Spatiotemporal Photopatterning on Polycarbonate Surface through Visible Light Responsive Polymer Bound DASA Compounds. *ACS Macro Lett.* **2015**, *4*, 1273–1277. [[CrossRef](#)]
20. Safar, P.; Povazanec, F.; Pronayova, N.; Baran, P.; Kickelbick, G.; Kosizek, J.; Breza, M. No Title. *Collect. Czech. Chem. Commun.* **2000**, *65*, 1911–1938.
21. Klajn, R. Spiropyran-Based Dynamic Materials. *Chem. Soc. Rev.* **2014**, *43*, 148–184. [[CrossRef](#)] [[PubMed](#)]
22. Lukyanov, B.S.; Lukyanova, M.B. Spiroyrans: Synthesis, Properties, and Application. (Review)*. *Chem. Heterocycl. Compd.* **2005**, *41*, 281–311. [[CrossRef](#)]

23. Saad, A.; Oms, O.; Marrot, J.; Dolbecq, A.; Hakouk, K.; El Bekkachi, H.; Jobic, S.; Deniard, P.; Dessapt, R.; Garrot, D.; et al. Design and Optical Investigations of a Spiro-naphthoxazine/Polyoxometalate/ Spiropyran Triad. *J. Mater. Chem. C* **2014**, *2*, 4748–4758. [[CrossRef](#)]
24. Wagner, K.; Robert, B.; Zanoni, M.; Gambhir, S.; Dennany, L.; Breukers, R.; Higgins, M.; Wagner, P.; Diamond, D.; Wallace, G.G.; et al. A Multiswitchable Poly(Terthiophene) Bearing a Spiropyran Functionality: Understanding Photo- and Electrochemical Control. *J. Am. Chem. Soc.* **2011**, *133*, 5453–5462. [[CrossRef](#)]
25. Goulet-Hanssens, A.; Utecht, M.; Mutruc, D.; Titov, E.; Schwarz, J.; Grubert, L.; Bléger, D.; Saalfrank, P.; Hecht, S. Electrocatalytic Z → E Isomerization of Azobenzenes. *J. Am. Chem. Soc.* **2017**, *139*, 335–341. [[CrossRef](#)]
26. Goulet-Hanssens, A.; Rietze, C.; Titov, E.; Abdullahu, L.; Grubert, L.; Saalfrank, P.; Hecht, S. Hole Catalysis as a General Mechanism for Efficient and Wavelength-Independent Z → E Azobenzene Isomerization. *Chem* **2018**, *4*, 1740–1755. [[CrossRef](#)]
27. Li, Z.; Zhou, Y.; Peng, L.; Yan, D.; Wei, M. A Switchable Electrochromism and Electrochemiluminescence Bifunctional Sensor Based on the Electro-Trigged Isomerization of Spiropyran/Layered Double Hydroxides. *Chem. Commun.* **2017**, *53*, 8862–8865. [[CrossRef](#)]
28. Garling, T.; Tong, Y.; Darwish, T.A.; Wolf, M.; Kramer Campen, R. The Influence of Surface Potential on the Optical Switching of Spiropyran Self Assembled Monolayers. *J. Phys. Condens. Matter* **2017**, *29*, 414002–414010. [[CrossRef](#)]
29. Areephong, J.; Logtenberg, H.; Browne, W.R.; Feringa, B.L. Symmetric Six-Fold Arrays of Photo- and Electrochromic Dithienylethene Switches. *Org. Lett.* **2010**, *12*, 2132–2135. [[CrossRef](#)]
30. Peters, A.; Branda, N.R. Electrochromism in Photochromic Dithienylcyclopentenes. *J. Am. Chem. Soc.* **2003**, *125*, 3404–3405. [[CrossRef](#)]
31. Lerch, M.M.; Wezenberg, S.J.; Szymanski, W.; Feringa, B.L. Unraveling the Photoswitching Mechanism in Donor-Acceptor Stenhouse Adducts. *J. Am. Chem. Soc.* **2016**, *138*, 6344–6347. [[CrossRef](#)]
32. Hemmer, J.R.; Poelma, S.O.; Treat, N.; Page, Z.A.; Dolinski, N.D.; Diaz, Y.J.; Tomlinson, W.; Clark, K.D.; Hooper, J.P.; Hawker, C.; et al. Tunable Visible and Near Infrared Photoswitches. *J. Am. Chem. Soc.* **2016**, *138*, 13960–13966. [[CrossRef](#)]
33. Lui, B.F.; Tierce, N.T.; Tong, F.; Sroda, M.M.; Lu, H.; Read de Alaniz, J.; Bardeen, C.J. Unusual Concentration Dependence of the Photoisomerization Reaction in Donor–Acceptor Stenhouse Adducts. *Photochem. Photobiol. Sci.* **2019**, *18*, 1587–1595. [[CrossRef](#)] [[PubMed](#)]
34. Liu, H.; Pu, S.; Liu, G.; Chen, B. Photochromism of Asymmetrical Diarylethenes with a Pyrimidine Unit: Synthesis and Substituent Effects. *Dye. Pigment.* **2014**, *102*, 159–168. [[CrossRef](#)]
35. Bull, J.N.; Carrascosa, E.; Mallo, N.; Scholz, M.S.; Da Silva, G.; Beves, J.E.; Bieske, E.J. Photoswitching an Isolated Donor-Acceptor Stenhouse Adduct. *J. Phys. Chem. Lett.* **2018**, *9*, 665–671. [[CrossRef](#)] [[PubMed](#)]